Published in final edited form as:
Ther Deliv. 2012 February ; 3(2): 181–194.

The shape of things to come: importance of design in nanotechnology for drug delivery

Yaling Liu[1,2,*], **Jifu Tan**[1], **Antony Thomas**[2], **Daniel Ou-Yang**[3], and **Vladimir R Muzykantov**[4]

[1]Department of Mechanical Engineering & Mechanics, Lehigh, University, Bethlehem, PA 18015, USA

[2]Bioengineering Program, Lehigh University, Bethlehem, PA 18015, USA

[3]Department of Physics, Lehigh University, Bethlehem, PA 18015, USA

[4]Institute for Translational Medicine & Therapeutics, Department of Pharmacology, University of Pennsylvania School of Medicine, PA, USA

Abstract

The design of nanoparticle (NP) size, shape and surface chemistry has a significant impact on their performance. While the influences of the particle size and surface chemistry on drug delivery have been studied extensively, little is known about the effect of particle shapes on nanomedicine. In this perspective article, we discuss recent progress on the design and fabrication of NPs of various shapes and their unique delivery properties. The shapes of these drug carriers play an important role in therapeutic delivery processes, such as particle adhesion, distribution and cell internalization. We envision that stimuli-responsive NPs, which actively change their shapes and other properties, might pave way to the next generation of nanomedicine.

Nanotechnology is the understanding and control of matters having dimensions roughly within the 1–100 nm range [201]. Various nanoparticle (NP)-based therapeutic platforms, including liposomes [1,2], polymeric micelles [3,4], quantum dots [5,6], Au/Si/polymer shells [7,8] and dendrimers [9,10] have been established. The aim of therapeutic delivery is to improve patient treatment by enabling the administration of new intricate drugs, improving the bioavailability of existing drugs and providing spatial and temporal targeting of drugs to reduce side effects and increase efficiency.

Carriers in the nanoscale offer the advantages of enhanced delivery efficiency, targeting, controlled release and ability to bypass biological barriers. NPs can be engineered into different sizes, shapes and surface chemistries to meet these requirements. As a key characteristic of NPs, size has been studied extensively and reported in the literature. For example, it is known that spherical particles bigger than 200 nm are efficiently filtered by liver, spleen and bone marrow, while particles smaller than 10 nm can be quickly cleared by the kidney or through extravasation, thus making 10–200 nm the ideal size range for the

*Author for correspondence: yal310@lehigh.edu.

Financial & competing interests disclosure

The authors acknowledge support of this work from National Science Foundation grants CBET-1113040, CBET-1067502, DMR-0923299 and NIH grant EB009786. The authors have no other relevant affiliations or financial involvement with any organization or entity with a financial interest in or financial conflict with the subject matter or materials discussed in the manuscript apart from those disclosed.

No writing assistance was utilized in the production of this manuscript.

circulating spherical carriers. Similar to size, shape is also a fundamental property of NPs that is critical for their intended biological functions. Most NPs have a spherical shape. With advanced nanofabrication techniques, different shapes and forms of NPs have emerged in recent years with unique geometrical, physical and chemical properties. For example, nanorods with suitable aspect ratios have been fabricated as a novel contrast agent for both molecular imaging and photothermal cancer therapy [11]; asymmetrically functionalized gold-NPs have been assembled to build nanochains [12]; superparamagnetic iron oxide-based nanoworms are studied for tumor targeting [13] and nanonecklaces are assembled using gold NPs by covalent bonding [14]. It has been reported that cylindrically shaped filamentous micelles can effectively evade nonspecific uptake by the reticulo-endothelial system, allowing persistent circulation for up to 1 week after intravenous injection [15]. In this article we will focus on how the variability in the shape and design of NPs influence their functionality.

Design considerations for NPs: size, shape & surface functionalization

Being the key parameters that influence the transport and adhesion of NPs, size and surface functionalization have been studied extensively [16]. Some general principles have been formulated to achieve a better performance of drug carriers. For example, NPs with a diameter less than 100 nm are considered ideal for tumor targeting via leaky vasculature [17].

The adhesion capability of NPs is heavily depended on the surface functionalities they have been decorated with. For nanorods, it is reported that Janus coating leads to better adhesion compared with uniform coating [18,19]. Protein adsorption, and the subsequent phagocytosis, of particles *in vivo* have been shown to be reduced by the immobilization of polyethylene glycol (PEG) on the particles [20]. Many studies apply PEG-based copolymer modifications, which enhance circulating half life, while contributing to a decreased uptake by nontarget cells. On the other hand, phage display-based targeting on various organs has been performed by the immobilization of specific peptides on NPs. Selective localization of bacteriophage to brain and kidney blood vessels were performed and showed an up to 13-fold selectivity for these organs [21].

NP-based drug delivery has also been performed using NP–aptamer bioconjugates. Here, NPs having rhodamine-labeled dextran were encapsulated in poly(lactic acid) (PLA)–PEG copolymer with a terminal carboxylic acid. The carboxylic acid functional group is modified with RNA aptamers that bind to the prostate-specific membrane antigen on prostate LNCaP epithelial cells. The surface charge on the NP was kept negative to minimize nonspecific interactions with the negatively charged nucleic acid aptamers. Carboxylic acid groups on the NP surface give the flexibility of bringing in many potential modifications through covalent conjugation [22]. Despite these successes, postsynthesis surface modification on NPs involves an excess amount of chemical reactants and reactions [23]. This is a hindrance towards accurately reproducing their biophysicochemical properties, introducing batch-to-batch variations. Using prefunctionalized biomaterials that self-assemble into targeted NPs would eliminate the need for postparticle modifications and produce precisely engineered NPs with a higher degree of reproducibility. Multicompartment micelles having a water-soluble shell and a segregated hydrophobic core are an approach towards eliminating postsynthesis modification [24]. Complex micelles with tunable channels are formed by the self-assembly of two diblock environmental stimuli-responsive copolymers, poly(tertbutyl acrylate) -b-poly(*N*-isopropylacrylamide) and poly(*tert*-butyl acrylate)-b-poly(4-vinyl-pyridine). The size and permeability of the channels are regulated by manipulating the composition of the diblock copolymers or by changing external stimuli factors, such as temperature, pH value and ionic strength [25]. Polymeric micelles constructed from PLA-b-

PEG-b-poly(L-histidine) (polyHis) having a flower-like assembly of PLA and polyHis blocks in the core and PEG block as the shell, have been applied as a pH-specific anticancer drug carrier. In a low-pH environment (characteristic of tumor and diseased-tissue environment), the transformation in the physical form of PLA-b-PEG-b-polyHis micelles leads to drug release from the micelles [26]. Similar pH sensitivity-triggered drug release mechanisms, based on a change in surface charge or degradation mechanism of the nanocarrier, have been investigated by other groups [27,28]. Complex and unusual nanometer-sized architectures have been fabricated, including a triblock copolymer consisting of a protein and a self-assembled synthetic diblock copolymer. The formation of the amphiphilic biohybrid macromolecule is driven by a processes of self-organization, involving radical polymerization, click chemistry and cofactor reconstitution [29].

Particles that mimic the geometry of red blood cells (RBCs) are fabricated using layer-by-layer self-assembly of bovine serum albumin (BSA) and poly(allylamine hydrochloride) (PAH). They demonstrate many key attributes of RBCs including size, shape, elastic modulus, ability to deform under flow and oxygen-carrying capacity [30]. Drug carriers having multifunctional targeting and imaging capabilities have been fabricated using particle lithography techniques, allowing a nanoscale precision for site-specific chemical modifications on the surface of colloidal NPs [31].

Multiple functionalities can be introduced at optimal locations on high-aspect-ratio NPs having a large surface area. Different metals are introduced at portions of the NPs, allowing selective functionalization and avoiding molecular interference *in vivo*, due to randomly distributed groups [32]. Multisegment bimetallic nanorods that can simultaneously bind to compact DNA plasmids and targeting ligands in a precisely spatially defined manner have been applied in gene-delivery systems [32]. Cell-targeting proteins (e.g., transferrins) are selectively attached to the gold segment of thenanorod, while the DNA plasmids to be delivered are attached to the nickel segment of the nanorod [32]. A detailed study of the controlled drug release has been conducted on silica-based mesoporous nanomaterials that have mesocaged cubic, cylindrical and tetragonal pore structures of different textural and morphological properties. Drug release rate can be controlled based on the 2D or 3D connectivities of the pores, pore geometries and particle size [33].

Despite these efforts on controlling NP size and surface properties, shape effect on NP performance has not gained much attention until recently. In this perspective article, we review how NPs' shape affects their binding, biodistribution and cellular uptake.

Shape diversity in nature: viruses & cells

Nanoscale creatures in nature display a variety of shapes. Viruses consist of a nucleic acid molecule inside a protein capsid and they replicate within the living cells of organisms. Viruses, usually much smaller than bacteria, have sizes ranging from 5 to 300 nm. They exhibit a variety of shapes, as shown in Figure 1, which can be classified into four categories:

- Helical viruses with rod-shaped or filamentous virions, which can be short and highly rigid, or long and very flexible. For example, the classic rod-shaped tobacco mosaic viruses have lengths of approximately 300 nm, cylindrical diameters of 18 nm and a helical pitch of 23 nm [34];
- Icosahedral viruses;
- Enveloped viruses, such as HIV;

- Complex viruses that possess a capsid that is neither purely helical nor icosahedral and that may possess extra structures, such as protein tails or a complex outer wall. For example, the helical tail of Enterobacteria phage T4, a type of cacteriophages, is used as a tube to inject DNA from the capsid into host cells [35].

Given such diversity, however, there are very few studies on why viruses attain so many different shapes and how different shapes influence their functions. The various sizes and shapes of viruses have motivated the development of NPs of different designs as drug carriers, as shown in Figure 2. In recent years, viral vectors, virus-like particles and virosomes have been proposed as drug carriers and imaging contrast-enhancing agents [36]. Viral vectors, especially adenoviral vectors, can produce high levels of gene expression for the treatment of heart failures [37].

Another microscopic structure with a notable shape is the RBC. RBCs are flexible biconcave disks that lack a cell nucleus and most other organelles, with a size of approximately 8 μm. They are capable of traversing biological barriers, which are impenetrable to objects less than one-tenth of their size, and manage to avoid clearance by macrophages for up to a few months. Highly deformable, they are capable of squeezing though blood vessels in the brain with a diameter of only approximately 2 μm [38]. The large volume and biocompatibility also distinguish RBCs as ideal drug carriers. For example, a fibrinolytic agent containing a tissue-type plasminogen activator conjugated to the RBC surface can dissolve nascent clots in a Trojan horse-like strategy, while having minimal side effects [39]. Animal-model studies suggests an RBC/tissue-type plasminogen activator could be used as a thromboprophylactic agent in patients [40]. It has also been reported that polymeric particles attached to rat RBCs circulate longer (over 10 h) than those not attached [41]. Deformability of RBC helps the long circulation. Highly deformable worm-shaped particles called filamicelles can effectively evade nonspecific uptake by the reticuloendothelial system, allowing persistent circulation for up to 1 week after intravenous injection [15]. It has recently been tested *in vivo* that hydrogel particles with smaller elastic modulus can bypass several organs, resulting longer circulation times compared with traditional rigid solid particles [42].

Fabrication of nonspherical NPs

Traditional NPs fabricated using bottom-up techniques are limited to spheres, partly due to the lack of fabrication technology to control the shape. Bottom-up techniques greatly involving self-assembly and aggregation of NPs depend on various factors, such as its thermodynamic energy minima and entropy limitations or factors affecting molecular self-assembly [43]. The energy-minimized stable structures thus produced tend to be spherical, because spheres have the least surface per unit volume and, thus, minimize the interfacial energies. The advancement of techniques involved in nanofabrication have enabled the development and production of various nonspherical NPs. Table 1 summarizes NPs of various shapes and properties that have been fabricated recently. Particle replication in non-wetting template (PRINT®) is a soft lithography technique for producing isolated NPs of various shapes, using perfluoropolyethers (PFPEs) as a template. PFPE forms a template containing cavities of the desired shape and size, which is pressed into a thin film of particle precursor polymer solution. The polymer is selectively filled into the cavities and solidified either by cross-linking or evaporation of solvent, forming NPs of specific shapes that can then be easily harvested. Taking advantages of PFPE, PRINT generates shape-specific NPs with high throughput [44–48].

A large variety of shapes can be achieved by embedding polystyrene spheres in a polymer film and stretching the film. This is achieved by adjusting parameters such as the aspect ratio of stretching, the thickness of the film or method used to liquefy the polystyrene

particles. Particle sizes range from less than 1–10 μm with the smallest size reported to be a few hundred nanometers and can be stretched into a high aspect ratio of approximately 20. With this technique, the quality of the starting spheres determines the uniformity of the shape and size of the final products [49,50].

Step-flash imprint lithography is a commercially available (Molecular Imprint®) nanoimprint process, which employs a quartz template technique very similar to soft lithography. Using the technique, cube-shaped particles as well as those having triangle- or pentagon-shape cross sections (≥50 nm) can be fabricated from cross-linkable PEG-based polymers with incorporated biofunctional agents. *In vitro* enzymetriggered release of antibodies and plasmid DNA from these NPs were also demonstrated [51].

As a cost-effective method, self-assembly has been widely used to spontaneously aggregate synthesized molecules to complex, hierarchically ordered composite structures [15,52]. Self-assembly liposomes have been developed to deliver antitumor drugs and have received clinical approval [53]. Basically, a self-assembly system consists of a group of components; for example, molecules that aggregate together mainly through a balance of attractive and repulsive interactions. These interactions are generally weak and noncovalent. Normally, self-assembly is carried out in a solution that enables the components to move easily.

Techniques have been reported that mimic the shape and properties of healthy and diseased RBCs. RBC-shaped template poly(lactic-co-glycolic acid) (PLGA) particles (7 ± 2 μm) are prepared from spherical PLGA particles of appropriate sizes using the electrohydrodynamic jetting process and incubating them in 2-propanol. Soft, protein-based biocompatible RBC-shaped particles were obtained from this template using layer-by-layer self-assembly of PAH/BSA or hemoglobin/BSA, being polycationic and polyanionic, respectively. After adsorption of nine alternate layers on the template, the shell was crosslinked using glutaraldehyde, and the PLGA core was removed using 1:2 2-propanol:tetrahydrofuran solution [30].

A template-induced printing technology has been developed to fabricate nonspherical polymeric particles with a variety of aspect ratios and local shapes [54,55]. Basically, a bi-layer structure made of SU-8 (Microchem®) or PEG diacrylate on top of a sacrificial layer, such as polymethylmethacrylate or polyvinyl alcohol, is exposed through a photomask to UV light. A proper solvent dissolves the unexposed polymers after exposure. This process has been used to fabricate 2–3-μm diameter PEG discs in a variety of thicknesses from 100, 200 to 500 nm with water as the solvent for releasing and harvesting the particles.

Shape has significant impact on almost every aspect of drug delivery. In the following sections, we review a few important processes and discuss the influence of NP shapes, respectively.

Adhesion & biodistribution

NPs have to bypass the reticulo-endothelial system and avoid the clearance by the spleen and liver before they reach the targeted disease sites. The size of the particles can play an important role in accumulation at diseased sites. The NPs used in nanomedicine usually range from 20 to 200 nm, because NPs larger than 200 nm are mechanically filtered in the spleen, while those smaller than 100 nm leave the blood vessels through fenestrations in the endothelial lining [56]. Microparticles are cleared by Kupffer cells in liver or physically trapped in the capillary beds [57]. For particles larger than 200 nm, deformability is required in order to navigate through the liver and spleen. Particularly, for the treatment of tumors and cancer, 100–200 nm NPs are attractive because of the unique feature known as the enhanced permeability and retention effect [58].

Similar to size, shape is a fundamental property of NPs that may be critically important for their intended biological functions [59–65]. Recent data reveal that particle shape may have a profound effect on their biological properties. For example, Discher's group found that the circulation of filomicelles can last up for 1 week in rodents, as shown in Figure 3 [15]. A few factors may contribute to the long circulation, such as length and flexibility. For flexible filomicelles, the optimal length is approximately 8 μm [36]. The same group found that prolonged circulating filomicelles loaded with drug paclitaxel can penetrate into the tumor stroma and produce greater and more sustained tumor shrinkage and tumor cell apoptosis [66]. Muzykantov's group also found that disk-shaped carriers targeted to intercellular adhesion molecule 1 had longer half-lives in circulation [67].

A few mathematical models have been developed to study the adhesion properties for NPs of various shapes. Considering buoyancy, hemodynamic forces, van der Waals, electrostatic and steric interactions, a study by Decuzzi and Ferrari concluded that particles used for drug delivery should have a radius smaller than 100 nm in order to facilitate their margination toward and interaction with the endothelium wall [68–70]. The same group also studied the adhesive strength of nonspherical particles based on a simplified mathematical model [68]. The proposed analytical formula for adhesion of nonspherical NPs is:

$$\frac{P_a}{m_r\, m_l\, K_a^0} = A_c \exp\left[-\frac{\lambda}{k_B\, T}\frac{F_{dis}}{m_r\, A_c}\right]$$

where K_a^0 is the association constant at zero load of the ligand–receptor pair, F_{dis} is the dislodging force due to hydrodynamic forces, m_r and m_l are the receptor and ligand density, respectively, A_c is contact area, λ is the characteristic length of the ligand–receptor bonds, k_B is the Boltzmann constant, and T is the absolute temperature. Normalized adhesion probability of oblate-, rod- and disc-shaped NPs for a wall shear stress of 1 Pascal is plotted as a function of particle volume in Figure 4 [71]. The aspect ratio of disc (diameter over thickness) and rod (length over diameter) are chosen to be five. The disk-shaped NPs are predicted to have the largest adhesion probability due to the large surface area available for contact.

Liu and colleagues used Brownian adhesion dynamics to study the binding dynamics of NPs from transport, margination, to adhesion [72,73]. It was found that rod-shaped NPs have higher binding rates compared with their spherical counterparts, due to the tumbling motion of NPs and larger adhesion area once upon contact. The typical trajectories of nanorods and nanospheres are shown in Figure 5. The computational modeling provides a practical guide to geometry considerations when designing nanoscale drug carriers.

Decuzzi and Ferrari's group also studied the effects of size and shape in the biodistribution of intravascularly injected silicon-based particles with diameters from 700 nm to 3 μm and with quasi-hemispherical, cylindrical and discoidal shapes [74]. It was observed that discoidal particles accumulate excessively in most organs but liver, as shown in Figure 6, which was probably due to the larger rotational inertia and surface of contact.

Cell internalization

NPs of different size and shape exhibit different cell internalization rates, which are confirmed by both computational modeling and *in vitro* and *in vivo* experiments experiments. Particle size plays a key role in cell internalization. It seems that particles with sizes above 5 μm will not be internalized by cells [75]. Comparing gold NPs with diameters of 14, 50 and 74 nm, Chithrani and Chan found significantly higher uptake for 50 nm

spherical particles [76]. Similar to size, shape also influences NP uptake. Yang and Ma used computer simulation to investigate translocation processes of NPs with different shapes [77]. While vesicular uptake such as phagocytosis and endocytosis are the major forms of cellular uptake processes, direct membrane penetration is assumed as the leading mechanism in the simulation. As shown in Figure 7, the translocation processes of nanospheres, nano-ellipsoids, nanorods, nanodiscs and pushpin-like NPs across a lipid bilayer were studied by dissipative particle dynamics. It was reported that the shape anisotropy and initial orientation of the particle are crucial to the interactions between the particle and lipid bilayer. The penetrating capability of a NP is influenced by the contact area between the particle and lipid bilayer and the local curvature of the particle at the contact point. Particle volume is also found to directly affect translocation processes.

Scanning electron microscope images have confirmed the uptake of discoidal silicon microparticles by J444A.1 cell macrophages, as shown in Figure 8 [78]. Muzykantov's group found that disk-shape carriers targeted to intercellular adhesion molecules 1 had higher targeting specificity in mice, whereas spherical ones were endocytosed more rapidly [67]. The Desimone group reported that high aspect ratio rod-like hydrogel particles (d = 150 nm, h = 450 nm) were internalized about four-times faster than the more symmetric cylindrical particle (d = 200 nm, h = 200 nm), although they have almost the same volume [79]. A possible explanation is the abundance of cells that high aspect ratio particles can interact through multivalent cationic interactions because of larger contact surface areas. To elucidate the shape effect on phagocytosis, Mitragotri's group studied alveolar macrophages of polystyrene particles of different sizes and shapes [80]. They found cells attached along the major axis of an elliptical disk internalizes it completely in 3 min while cells attached to the flat side of an identical elliptical disk spreads, but does not internalize the particle [81]. They pointed out that the orientation of the particles measured by tangent angles at the first point of contact determines whether macrophages initiate phagocytosis or simply spread particles. This finding is also supported by computer simulation of the NP transportation through the membrane [77]. Thus, by engineering the shape of NPs, phagocytosis could be actively promoted or prevented.

Drug loading & release

To take advantage of NPs as therapeutic carriers, a drug has to be loaded into and released from NPs. Multiple emulsion techniques have been used to encapsulate drugs into polymer nanocarriers [81–83]. Drug load capacity depends on the size, shape and structure of the nanocarriers. It is reported that nonspherical particles such as filomicelles have much higher drug-load capacity compared with spherical counterparts [84]. This is because while filamentous particles have one-dimension in nanoscale, the other dimensions could be expanded to load more drugs. For silicon NPs, hollow-core and mesoporous shell structures have been designed to load drug molecules [85]. Pore size, surface potential and hydrophilicity can also be changed to increase drug-loading capacity [86,87]. Drug-loaded nanocarriers can be transported and adhered on targeted cells through ligand–receptor binding [88]. After cell internalization, a drug may be released by diffusion, drug-carrier swelling or erosion, depending on the drug solubility and carriers' solubility and resistance to erosion [89,90]. For example, due to the biocompatibility and biodegradability, drug encapsulated in PLGAbased nanocarriers enable the drug to be released at a constant rate through diffusion [83]. With the same volume, nonspherical particles have a larger surface area than the spherical particles, giving rise to a larger drug flux per unit volume. Controlled drug release from porous NPs has been achieved through pH-responsive release, nanocaps and nanovalves release under external stimuli. For example, Zhu *et al.* reported a pH-responsive release by coating polyelectrolyte (PAH/poly sodium styrenesulfonate) multilayers on hollow silica NPs [91]; Thomas *et al.* applied an alternating current magnetic

field to generate internal heating to disassemble the thermally sensitive gatekeeper and release the drug [92]. Mal *et al.* designed coumarin-modified mesoporous silica drug carrier to release guest molecules through photoactive derivatives [93].

Future perspective

An emerging NP design in the future is to devise NPs that can actively change shape and properties based on their local environment. Success of these efforts could significantly improve biological specificity in diagnosis and therapies through a precise spatiotemporal control of agent delivery. To achieve this goal, continuous efforts have been dedicated to the development of stimuli-responsive nanoplatforms. Various environmental stimuli including pH [94], temperature [95], enzymatic expression [96], redox reaction [97] and light [98] have been studied. For example, while rod-shaped particles are easier to reach the target site, the uptake process is slower compared with their spherical counterparts. If NPs could be designed to change shape once they reach the disease site, the delivery efficiency could be improved. There have been certain efforts toward this direction. For example, pH- and heat-sensitive NPs have been created to target tumor sites [99]. Self-assembled core/shell NPs that display a pH-sensitive thermal response have recently been reported. The NPs were encapsulated with the anticancer drug doxorubicin, whose release was pH dependent, which was found to enter the nucleus more rapidly than those transported by non-pH-sensitive NPs. Zhou *et al.* reported a set of tunable, pH-activatable micellar NPs based on the supramolecular self-assembly of ionizable block copolymer micelles [94]. Yang *et al.* reported formation of shape-switching main-chain liquid crystalline polymer NPs using a mini emulsion technique [100]. The NPs are naturally ellipsoidal with a high aspect ratio, which changes reversibly to the spherical shape upon heating. Degradable PEG-based hydrogel microparticles have been fabricated using stop-flow lithography producing particles of independently tunable size, shape, and erosion profile. High design flexibility is endowed by the single hydrogel microparticles having multiple distinct degradation regions with custom erosion profiles performing targeted delivery [101]. Real-time changes in the shape of elongated PLGA NPs to spheres were performed by modulating the subtle balance between polymer viscosity and interfacial tension by external stimuli, such as temperature, pH or chemical additives [102]. Elongated rod-like or elliptical disk-like NPs, as shown in Figure 9, can efficiently target tumors because of their prolonged circulation. On reaching the tumor site, the NP actively shifts its shape to be spherical, facilitating cell internalization, thus leading to more efficient tumor treatment [103].

It has been reported that worm-shaped polymers have a long circulating life but poor adhesion properties. Smarter designs aimed at breaking the dilemma have not yet been achieved. Recently, the poor adhesion of worm-shaped polymers has been improved by anchoring antibodies, which recognize distinct endothelia surface molecules [103]. Results showed antibody-targeted filomicelles can retain both the structural integrity and dynamic flexibility, and adhere to endothelium with high specificity both *in vitro* and *in vivo*. Based on an all-atom molecular dynamics simulation, a rational coarse grain model of nanoworms and nanospheres has been generated to study the shape-dependent effects on drug delivery. The simulation results showed that worm-shaped particles exhibit enhanced drug release compared with spherical ones [84]. Similar *in vitro* and *in vivo* studies are required to investigate how drug-loaded micelles interact with the cell membranes. Studies must also be made to investigate if the change in drug shape facilitates drug diffusion across the micellar interface to the cell membrane. Another possibility is to use external stimuli such as pH or temperature to break up the worm-like polymer so that it will dissemble into smaller drug carriers on site. The smaller size of the drug carriers will enhance its diffusion and uptake. It seems that if we could use pH- or temperature- sensitive crosslinkers as glue, we could break the links and change NP shape upon activation by pH or temperature. For example, a

new responsive nanocomposite material consisting of a poly-(*N*-isopropylacrylamide) hydrogel and 'super-crosslinking' silica NPs has been synthesized [104] by mixing both components in a solution, followed by spin coating on a thin film and photocrosslinking by UV irradiation. We should also consider shape-changing NPs be triggered enzymatically by the disease condition, leading towards better cellular uptake and enhanced drug dispersion. Other 'smart NPs' of different shapes, which enzymatically degrade to release the drug [51] have been discussed in this perspective article.

Another aspect that has rarely been discussed is the *in vivo* tolerance of the fabricated NPs. One critical question is whether *in vivo* swelling of the NPs, that is, hydrogel-based micro- and nano-scale drug carriers, could considerably alter their geometry to a point where the potential benefit of controlling the size or shape could be realized. Caldorera-Moore *et al.* measured the swelling ratio of NPs by atomic force microscopy and environmental scanning electron microscope capsules [105]. The swelling behavior of nano-imprinted hydrogel particles of different sizes and aspect ratios were characterized. Their results indicate a size-dependent swelling, which can be attributed to the effect of substrate constraint of as-fabricated particles, when the particles were still attached to the imprinting substrate. Both experimental and theoretical results suggest that hydrogel swelling does not significantly alter the shape and size of highly crosslinked nanoscale hydrogel particles used in the present study.

In summary, shape plays an important role in various processes that determines NP targeted drug-delivery efficiency. Engineering drug carriers into various shapes need combined efforts of theoretical prediction, nanofabrication and *in vitro* and *in vivo* testing. While we have observed a significant progress in engineering design of NPs, the shape of things is yet to reveal its true potentials for applications in nanomedicine.

Key Terms

Reticulo-endothelial system	The same as mononuclear phagocyte system, it consists of the phagocytic cells located in reticular connective tissue
Phagocytosis	Engulfing and ingestion of bacteria or other foreign bodies by phagocytes
Thromboprophylaxis	Prevention of or protective treatment to prevent coronary thrombosis
Enhanced permeability and retention effect	Certain sizes of molecules (typically liposomes, nanoparticles and macromolecular drugs) tend to accumulate in tumor tissue much more than they do in normal tissues
Margination	The lateral drift of particles toward the endothelial walls
Stimuli-responsive nanoplatform	Smart nanocarriers that can control drug release through external stimuli, such as pH, temperature, light and magnetic field

References

Papers of special note have been highlighted as:

- ■ of interest
- ■■ of considerable interest

1. Samad A, Sultana Y, Aqil M. Liposomal drug delivery systems: an update review. Curr Drug Deliv. 2007; 4(4):297–305. [PubMed: 17979650]
2. Sharma G, Anabousi S, Ehrhardt C, Ravi Kumar MN. Liposomes as targeted drug delivery systems in the treatment of breast cancer. J Drug Target. 2006; 14(5):301–310. [PubMed: 16882550]
3. Sutton D, Nasongkla N, Blanco E, Gao J. Functionalized micellar systems for cancer targeted drug delivery. Pharm Res. 2007; 24(6):1029–1046. [PubMed: 17385025]
4. Torchilin VP. Targeted polymeric micelles for delivery of poorly soluble drugs. Cell Mol Life Sci. 2004; 61(19–20):2549–2559. [PubMed: 15526161]
5. Gao X, Yang L, Petros JA, Marshall FF, Simons JW, Nie S. *In vivo* molecular and cellular imaging with quantum dots. Curr Opin Biotechnol. 2005; 16(1):63–72. [PubMed: 15722017]
6. Smith AM, Ruan G, Rhyner MN, Nie S. Engineering luminescent quantum dots for *in vivo* molecular and cellular imaging. Ann Biomed Eng. 2006; 34(1):3–14. [PubMed: 16450199]
7. Koenig S, Chechik V. Shell cross-linked Au nanoparticles. Langmuir. 2006; 22(11):5168–5173. [PubMed: 16700609]
8. Lou X, Wang C, He L. Core-shell Au nanoparticle formation with DNA-polymer hybrid coatings using aqueous ATR. Biomacromolecules. 2007; 8(5):1385–1390. [PubMed: 17465524]
9. Duncan R, Izzo L. Dendrimer biocompatibility and toxicity. Adv Drug Deliv Rev. 2005; 57(15): 2215–2237. [PubMed: 16297497]
10. Najlah M, D'Emanuele A. Crossing cellular barriers using dendrimer nanotechnologies. Curr Opin Pharmacol. 2006; 6(5):522–527. [PubMed: 16890022]
11. Huang X, El-Sayed IH, Qian W, El-Sayed MA. Cancer cell imaging and photothermal therapy in the near-infrared region by using gold nanorods. J Am Chem Soc. 2006; 128(6):2115–2120. [PubMed: 16464114]
12. Sardar R, Shumaker-Parry JS. Asymmetrically functionalized gold nanoparticles organized in one-dimensional chains. Nano Lett. 2008; 8(2):731–736. [PubMed: 18269261]
13. Park JH, von Maltzahn G, Zhang L, et al. Systematic surface engineering of magnetic nanoworms for *in vivo* tumor targeting. Small. 2009; 5(6):694–700. [PubMed: 19263431]
14. Dai Q, Worden JG, Trullinger J, Huo Q. A 'nanonecklace' synthesized from monofunctionalized gold nanoparticles. J Am Chem Soc. 2005; 127(22):8008–8009. [PubMed: 15926813]
15■■. Geng Y, Dalhaime P, Cai S, et al. Shape effects of filaments versus spherical particles in flow and drug delivery. Nat Nanotechnol. 2007; 2(4):249–255. Filaments show long circulation compared with spherical ones. [PubMed: 18654271]
16. Simone EA, Dziubla TD, Muzykantov VR. Polymeric carriers: role of geometry in drug delivery. Expert Opin Drug Deliv. 2008; 5(12):1283–1300. [PubMed: 19040392]
17. Alexis F, Pridgen E, Molnar LK, Farokhzad OC. Factors affecting the clearance and biodistribution of polymeric nanoparticles. Mol Pharm. 2008; 5(4):505–515. [PubMed: 18672949]
18. Chen HY, Yang M, Wang X, Tan LH, Chen H. Controlled assembly of eccentrically encapsulated gold nanoparticles. J Am Chem Soc. 2008; 130(36):11858–11859. [PubMed: 18707100]
19. Dormidontova EE, Djohari H. Kinetics of nanoparticle targeting by dissipative particle dynamics simulations. Biomacromolecules. 2009; 10(11):3089–3097. [PubMed: 19894765]
20. Gref R, Minamitake Y, Peracchia MT, Trubetskoy V, Torchilin V, Langer R. Biodegradable long-circulating polymeric nanospheres. Science. 1994; 263(5153):1600–1603. [PubMed: 8128245]
21. Pasqualini R, Ruoslahti E. Organ targeting *in vivo* using phage display peptide libraries. Nature. 1996; 380(6572):364–366. [PubMed: 8598934]
22. Farokhzad OC, Jon S, Khademhosseini A, Tran TN, Lavan DA, Langer R. Nanoparticle-aptamer bioconjugates. Cancer Res. 2004; 64(21):7668–7672. [PubMed: 15520166]
23. Cheng J, Teply BA, Sherifi I, et al. Formulation of functionalized PLGA-PEG nanoparticles for *in vivo* targeted drug delivery. Biomaterials. 2007; 28(5):869–876. [PubMed: 17055572]
24. Kubowicz S, Baussard JF, Lutz JF, Thünemann AF, von Berlepsch H, Laschewsky A. Multicompartment micelles formed by self-assembly of linear ABC triblock copolymers in aqueous medium. Angewandte Chem Int Ed. 2005; 44(33):5262–5265.

25. Li G, Shi L, Ma R, An Y, Huang N. Formation of complex micelles with double-responsive channels from self-assembly of two diblock copolymers. Angewandte Chem Int Ed. 2006; 45(30): 4959–4962.
26. Lee ES, Oh KT, Kim D, Youn YS, Bae YH. Tumor pH-responsive flower-like micelles of poly(L-lactic acid)-b-poly(ethylene glycol)-b-poly(L-histidine). J Control Release. 2007; 123(1):19–26. [PubMed: 17826863]
27. Oh KT, Kimb D, Youc HH, Ahnc YS, Lee ES. pH-sensitive properties of surface charge-switched multifunctional polymeric micelle. Int J Pharm. 2009; 376(1–2):134–140. [PubMed: 19394414]
28. Guo X, Szoka FC. Steric stabilization of fusogenic liposomes by a low-pH sensitive PEG—diortho ester—lipid conjugate. Biocon Chem. 2001; 12(2):291–300.
29. Reynhout IC, Cornelissen JJ, Nolte RJM. Self-assembled architectures from biohybrid triblock copolymers. J Am Chem Soc. 2007; 129(8):2327–2332. [PubMed: 17274615]
30. Doshi N, Zahra AS, Bhaskarb S, Lahannb J, Mitragotria S. Red blood cell-mimicking synthetic biomaterial particles. Proc Natl Acad Sci USA. 2009; 106(51):21495–21499. [PubMed: 20018694]
31. Yake AM, Zahr AS, Jerri HA, Pishko MV, Velegol D. Localized functionalization of individual colloidal carriers for cell targeting and imaging. Biomacromolecules. 2007; 8(6):1958–1965. [PubMed: 17477569]
32. Salem AK, Searson PC, Leong KW. Multifunctional nanorods for gene delivery. Nat Mater. 2003; 2(10):668–671. [PubMed: 12970757]
33. Strømme M, Brohede U, Atluri R, Garcia- Bennett AE. Mesoporous silica-based nanomaterials for drug delivery: evaluation of structural properties associated with release rate. Wiley Interdiscip Rev Nanomed Nanobiotechnol. 2009; 1(1):140–148. [PubMed: 20049785]
34. Kuznetsov YG, Malkin AJ, Lucas RW, Plomp M, McPherson A. Imaging of viruses by atomic force microscopy. J Gen Virol. 2001; 82(9):2025–2034. [PubMed: 11514711]
35. Rossmann MG, Mesyanzhinov VV, Arisaka F, Leiman PG. The bacteriophage T4 DNA injection machine. Curr Opin Struct Biol. 2004; 14(2):171–180. [PubMed: 15093831]
36. Yoo J-W, Irvine DJ, Discher DE, Mitragotri S. Bio-inspired, bioengineered and biomimetic drug delivery carriers. Nat Rev Drug Discov. 2011; 10(7):521–535. [PubMed: 21720407]
37. Rapti K, Chaanine AH, Hajjar RJ. Targeted gene therapy for the treatment of heart failure. Can J Cardiol. 27(3):265–283. [PubMed: 21601767]
38■■. Petros RA, DeSimone JM. Strategies in the design of nanoparticles for therapeutic applications. Nat Rev Drug Discov. 2010; 9(8):615–627. Excellent review on particle design. [PubMed: 20616808]
39. Murciano J-C, Medinilla S, Eslin D, Atochina E, Cines DB, Muzykantov VR. Prophylactic fibrinolysis through selective dissolution of nascent clots by tPA-carrying erythrocytes. Nat Biotechnol. 2003; 21(8):891–896. [PubMed: 12845330]
40. Danielyan K, Ganguly K, Ding BS, et al. Cerebrovascular thromboprophylaxis in mice by erythrocyte-coupled tissue-type plasminogen activator. Circulation. 2008; 118(14):1442–1449. [PubMed: 18794394]
41. Chambers E, Mitragotri S. Prolonged circulation of large polymeric nanoparticles by noncovalent adsorption on erythrocytes. J Control Release. 2004; 100(1):111–119. [PubMed: 15491815]
42. Merkel TJ, Herlihy K. Using mechanobiological mimicry of red blood cells to extend circulation times of hydrogel microparticles. Proc Natl Acad Sci USA. 2011; 108(2):586–591. [PubMed: 21220299]
43. Kazmaier NC. Bridging size scales with self assembling supramolecular materials. MRS Bull. 2000; 25:30–30.
44. Rolland JP, Hagberg EC, Denison GM, Carter KR, De Simone JM. High-resolution soft lithography: enabling materials for nanotechnologies. Angewandte Chem Int Ed. 2004; 43(43): 5796–5799.
45. Canelas DA, Herlihy K, DeSimone JM. Top-down particle fabrication: control of size and shape for diagnostic imaging and drug delivery. Wiley Interdiscip Rev Nanomed Nanobiotechnol. 2009; 1(4):391–404. [PubMed: 20049805]

46. Truong TT, Lin R, Jeon S, et al. Soft lithography using acryloxy perfluoropolyether composite stamps. Langmuir. 2007; 23(5):2898–2905. [PubMed: 17261048]
47. Rolland JP, Maynor BW, Euliss LE, Exner AE, Denison GM, DeSimone JM. Direct fabrication and harvesting of monodisperse, shape-specific nanobiomaterials. J Am Chem Soc. 2005; 127(28): 10096–10100. [PubMed: 16011375]
48. Gratton SE, Pohlhaus PD, Lee J, et al. Nanofabricated particles for engineered drug therapies: a preliminary biodistribution study of PRINT(TM) nanoparticles. J Control Release. 2007; 121(1–2):10–18. [PubMed: 17643544]
49. Champion JA, Katare YK, Mitragotri S. Making polymeric micro- and nanoparticles of complex shapes. Proc Natl Acad Sci USA. 2007; 104(29):11901–11904. [PubMed: 17620615]
50. Champion JA, Katare YK, Mitragotri S. Particle shape: a new design parameter for micro- and nanoscale drug delivery carriers. J Control Release. 2007; 121(1–2):3–9. [PubMed: 17544538]
51. Glangchai LC, Caldorera-Moore M, Shi L, Roy K. Nanoimprint lithography based fabrication of shape-specific, enzymatically-triggered smart nanoparticles. J Control Release. 2008; 125(3):263–272. [PubMed: 18053607]
52. Whitesides GM, Boncheva M. Beyond molecules: self-assembly of mesoscopic and macroscopic components. Proc Natl Acad Sci USA. 2002; 99(8):4769–4774. [PubMed: 11959929]
53. Drummond DC, Meyer O, Hong K, Kirpotin DB, Papahadjopoulos D. Optimizing liposomes for delivery of chemotherapeutic agents to solid tumors. Pharm Rev. 1999; 51(4):691–744. [PubMed: 10581328]
54■. Tao L, Zhao XM, Gao JM, Hu W. Lithographically defined uniform worm-shaped polymeric nanoparticles. Nanotechnology. 2010; 21(9):095301. Excellent reivew on microfabrication technique on nanoparticles. [PubMed: 20110578]
55. Tao L, Crouch A, Yoon F, et al. Surface energy induced patterning of organic and inorganic materials on heterogeneous Si surfaces. J Vac Sci Technol B. 2007; 25(6):1993–1997.
56. Stolnik S, Illum L, Davis SS. Long circulating microparticulate drug carriers. Adv Drug Deliv Rev. 1995; 16(2–3):195–214.
57. Mitragotri S, Lahann J. Physical approaches to biomaterial design. Nat Mater. 2009; 8(1):15–23. [PubMed: 19096389]
58. Huang S-D. Stealth nanoparticles: high density but sheddable PEG is a key for tumor targeting. J Control Release. 2010; 145(3):178–181. [PubMed: 20338200]
59. Devika B, Ghazani AA, Chan WC. Determining the size and shape dependence of gold nanoparticle uptake into mammalian cells. Nano Lett. 2006; 6(4):662–668. [PubMed: 16608261]
60. Lee H, Hoang B, Reilly RM, Allen C. The effects of particle size and molecular targeting on the intratumoral and subcellular distribution of polymeric nanoparticles. Mol Pharm. 2010; 7(4):1195–1208. [PubMed: 20476759]
61. Haun JB, Hammer DA. Quantifying nanoparticle adhesion mediated by specific molecular interactions. Langmuir. 2008; 24(16):8821–8832. [PubMed: 18630976]
62. Nishiyama N. Nanomedicine: nanocarriers shape up for long life. Nat Nanotechnol. 2007; 2:203–204. [PubMed: 18654260]
63. Ferrari M. Nanogeometry: beyond drug delivery. Nat Nanotechnol. 2008; 3:131–132. [PubMed: 18654480]
64. Cai S, Vijayan K, Cheng D, Lima EM, Discher DE. Micelles of different morphologies – advantages of worm-like filomicelles of PEO–PCL in paclitaxel delivery pharmaceutical research. 2008; 24(11):2099–2109.
65. Shinde Patil VR, Campbell CJ, Yun YH, Slack SM, Goetz DJ. Particle diameter influences adhesion under flow. Biophys J. 2001; 80(4):1733–1743. [PubMed: 11259287]
66. Christian DA, Cai S, Garbuzenko OB, et al. Flexible filaments for *in vivo* imaging and delivery: persistent circulation of filomicelles opens the dosage window for sustained tumor shrinkage. Mol Pharm. 2009; 6(5):1343–1352. [PubMed: 19249859]
67. Muro S, Garnacho C, Champion JA, et al. Control of endothelial targeting and intracellular delivery of therapeutic enzymes by modulating the size and shape of ICAM-1-targeted carriers. Mol Ther. 2008; 16(8):1450–1458. [PubMed: 18560419]

68■. Decuzzi P, Ferrari M. The adhesive strength of non-spherical particles mediated by specific interactions. Biomaterials. 2006; 27(30):5307–5314. Mathematical binding probability is provided for nonspherical particles. [PubMed: 16797691]

69. Decuzzi P, Lee S, Bhushan B, Ferrari M. A theoretical model for the margination of particles within blood vessels. Ann Biomed Eng. 2005; 33(2):179–190. [PubMed: 15771271]

70. Decuzzi P, Lee S, Decuzzi M, Ferrari M. Adhesion of microfabricated particles on vascular endothelium: a parametric analysis. Ann Biomed Eng. 2004; 32(6):793–802. [PubMed: 15255210]

71. Tao L, Hu W, Liu Y, Huang G, Sumer BD, Gao J. Shape-specific polymeric nanomedicine: emerging opportunities and challenges. Exp Biol Med. 2011; 236(1):20–29.

72■■. Shah S, Liu Y, Hu W, Gao J. Modeling particle shape-dependent dynamics in nanomedicine. J Nanosci Nanotechnol. 2011; 11(2):919–928. Numerical simulations on transport and adhesion dynamics of nanospheres and nanorods. [PubMed: 21399713]

73. Tan J, Thomas A, Liu Y. Influence of red blood cells on nanoparticle targeted delivery in microcirculation. Soft Matter. 2011 (Epub ahead of print). 10.1039/c2sm06391c

74■. Decuzzi P, Godin B, Tanaka T, et al. Size and shape effects in the biodistribution of intravascularly injected particles. J Control Release. 2010; 141(3):320–327. One of the few papers studying the shape effect on biodistribution. [PubMed: 19874859]

75. Wang J, Byrne JD, Napier ME, DeSimone JM. More effective nanomedicines through particle design. Small. 2011; 7(14):1919–1931. [PubMed: 21695781]

76. Chithrani BD, Chan WC. Elucidating the mechanism of cellular uptake and removal of protein-coated gold nanoparticles of different sizes and shapes. Nano Lett. 2007; 7(6):1542–1550. [PubMed: 17465586]

77. Yang K, Ma YQ. Computer simulation of the translocation of nanoparticles with different shapes across a lipid bilayer. Nat Nano. 2010; 5(8):579–583.

78. Serda RE, Mack A, Pulikkathara M, et al. Drug delivery: cellular association and assembly of a multistage delivery system. Small. 2010; 6(12):1329–1340. [PubMed: 20517877]

79. Gratton SE, Ropp PA, Pohlhaus PD, et al. The effect of particle design on cellular internalization pathways. Proc Natl Acad Sci USA. 2008; 105(33):11613–11618. [PubMed: 18697944]

80. Champion JA, Mitragotri S. Role of target geometry in phagocytosis. Proc Natl Acad Sci USA. 2006; 103(13):4930–4934. [PubMed: 16549762]

81. Lamprecht A, Ubrich N, Hombreiro Pérez M, Lehr C, Hoffman M, Maincent P. Biodegradable monodispersed nanoparticles prepared by pressure homogenizationemulsification. Int J Pharm. 1999; 184(1):97–105. [PubMed: 10425355]

82. Pandey R, Zahoor A, Sharma S, Khuller GK. Nanoparticle encapsulated antitubercular drugs as a potential oral drug delivery system against murine tuberculosis. Tuberculosis. 2003; 83(6):373–378. [PubMed: 14623168]

83. Orive G, Hernández RM, Gascón AR, Pedraz JL. Micro and nano drug delivery systems in cancer therapy. Cancer Ther. 2005; 3:131–128.

84. Loverde SM, Klein ML, Discher DE. Nanoparticle shape improves delivery: rational coarse grain molecular dynamics (rCG-MD) of Taxol in worm-like PEG–PCL micelles. Adv Mat. 2011 (Epub ahead of print). 10.1002/adma.201103192

85. He Q, Shi J. Mesoporous silica nanoparticle based nano drug delivery systems: synthesis, controlled drug release and delivery, pharmacokinetics and biocompatibility. J Mat Chem. 2011; 21(16):5845–5855.

86. Torney F, Trewyn BG, Lin V, Wang K. Mesoporous silica nanoparticles deliver DNA and chemicals into plants. Nat Nano. 2007; 2(5):295–300.

87. Meng H, Liong M, Xia T, et al. Engineered design of mesoporous silica nanoparticles to deliver doxorubicin and P-glycoprotein siRNA to overcome drug resistance in a cancer cell line. ACS Nano. 2010; 4(8):4539–4550. [PubMed: 20731437]

88. Martin CR, Kohli P. The emerging field of nanotube biotechnology. Nat Rev Drug Discov. 2003; 2(1):29–37. [PubMed: 12509757]

89. Arifin DY, Lee LY, Wang CH. Mathematical modeling and simulation of drug release from microspheres: implications to drug delivery systems. Adv Drug Deliv Rev. 2006; 58(12–13): 1274–1325. [PubMed: 17097189]

90. Grassi M, Grassi G. Mathematical modelling and controlled drug delivery: matrix systems. Curr Drug Deliv. 2005; 2(1):97–116. [PubMed: 16305412]

91. Zhu Y, Shi J, Shen W, et al. Stimuli-responsive controlled drug release from a hollow mesoporous silica sphere/polyelectrolyte multilayer core-shell structure. Angewandte Chem Int Ed. 2005; 44(32):5083–5087.

92. Thomas CR, Ferris DP, Lee JH, et al. Noninvasive remote-controlled release of drug molecules *in vitro* using magnetic actuation of mechanized nanoparticles. J Am Chem Soc. 2010; 132(31): 10623–10625. [PubMed: 20681678]

93. Mal NK, Fujiwara M, Tanaka Y. Photocontrolled reversible release of guest molecules from coumarin-modified mesoporous silica. Nature. 2003; 421(6921):350–353. [PubMed: 12540896]

94. Zhou K, Wang Y, Huang X, Luby-Phelps K, Sumer BD, Gao J. Tunable, ultrasensitive pH-responsive nanoparticles targeting specific endocytic organelles in living cells. Angewandte Chem Int Ed. 2011; 50(27):6109–6114.

95. Choi S-W, Zhang Y, Xia Y. A temperature-sensitive drug release system based on phase-change materials. Angewandte Chem. 2010; 122(43):8076–8080.

96. Wang C, Chen Q, Wang Z, Zhang X. An enzyme-responsive polymeric superamphiphile. Angewandte Chem Int Ed. 2010; 49(46):8612–8615.

97. Li YL, Zhu L, Liu Z, et al. Reversibly stabilized multifunctional dextran nanoparticles efficiently deliver doxorubicin into the nuclei of cancer cells. Angewandte Chem Int Ed. 2009; 48(52):9914–9918.

98. Febvay S, Marini DM, Belcher AM, Clapham DE. Targeted cytosolic delivery of cell-impermeable compounds by nanoparticle-mediated, light-triggered endosome disruption. Nano Lett. 2010; 10(6):2211–2219. [PubMed: 20446663]

99. Soppimath KS, Liu L-H, Seow WY, et al. Multifunctional core/shell nanoparticles self-assembled from pH-induced thermosensitive polymers for targeted intracellular anticancer drug delivery. Adv Funct Mat. 2007; 17(3):355–362.

100. Yang Z, Huck WT, Clarke SM, Tajbakhsh AR, Terentjev EM. Shape-memory nanoparticles from inherently non-spherical polymer colloids. Nat Mater. 2005; 4(6):486–490. [PubMed: 15895098]

101. Hwang DK, Oakey J, Toner M, et al. Stop-flow lithography for the production of shape-evolving degradable microgel particles. J Am Chem Soc. 2009; 131(12):4499–4504. [PubMed: 19215127]

102■■. Yoo J-W, Mitragotri S. Polymer particles that switch shape in response to a stimulus. Proc Natl Acad Sci USA. 2010; 107(25):11205–11210. Particles switch shape in response to temperature, pH or chemical additives. [PubMed: 20547873]

103. Shuvaev VV, Ilies MA, Simone E, et al. Endothelial targeting of antibody-decorated polymeric filomicelles. ACS Nano. 2011; 5(9):6991–6999. [PubMed: 21838300]

104. van den Brom CR, Anac I, Roskamp RF, et al. The swelling behaviour of thermoresponsive hydrogel/silica nanoparticle composites. J Mat Chem. 2010; 20(23):4827–4839.

105. Caldorera-Moore M, Kang MK, Moore Z, et al. Swelling behavior of nanoscale, shape- and size-specific, hydrogel particles fabricated using imprint lithography. Soft Matter. 2011; 7(6):2879–2887.

106. Briggs JA, Grünewald K, Glass B, Förster F, Kräusslich HG, Fuller SD. The mechanism of HIV-1 core assembly: insights from three-dimensional reconstructions of authentic virions. Structure. 2006; 14(1):15–20. [PubMed: 16407061]

Website

201. NIH. Nanotechnology. www.nih.gov/science/nanotechnology

Executive summary

- Size, shape and surface functionalization of particles have a profound impact on particle transport, adhesion and biodistritubion, which is verified by both mathematical modeling and experiments.
- Bioinspired and biomimicking drug platforms, including red blood cell-mimicking particles, viral vectors and virus-like particles could benefit nanomedicine designs.
- Different microfabrication techniques make it possible to fabricate particles with precise control on size and shape.
- Smart particles that actively change size and shape based on its local environment (pH, temperature and light) could revolutionize nanomedicine.

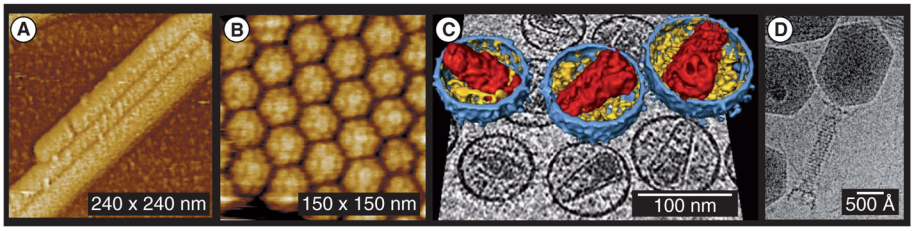

Figure 1. Viruses with different shapes

(A) Cylindrical helical virus; **(B)** Brome mosaic virus exhibits icosahedral symmetry; **(C)** HIVs with enveloped membrane; and **(D)** the complex shape of phage T4.

(A and B) Reprinted with permission from [34]. © Society for General Microbiology (2001).

(C) Reprinted with permission from [106]. © Elsevier (2006).

(D) Reprinted with permission from [35]. © Elsevier (2004).

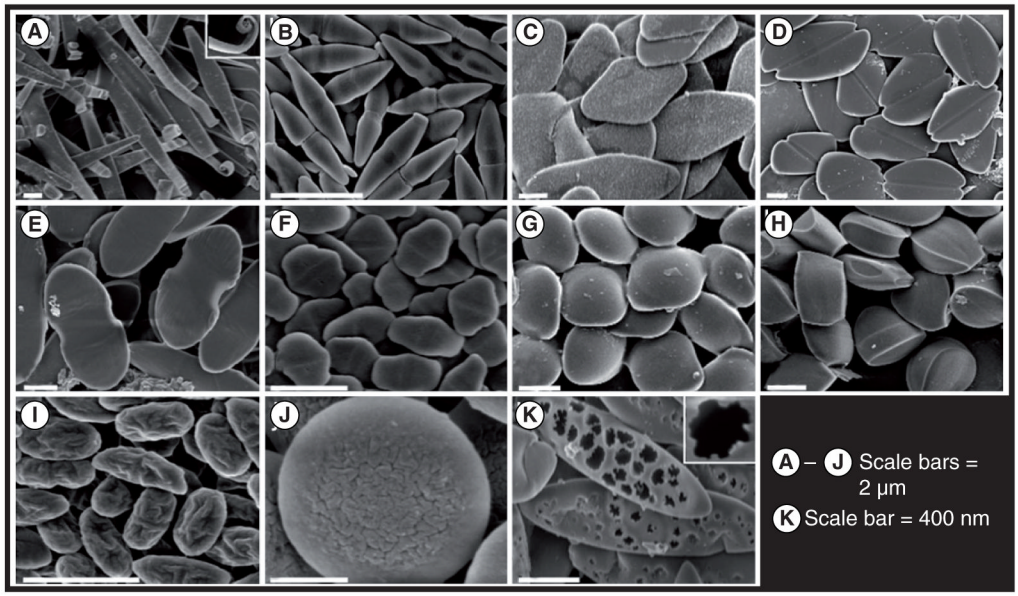

Figure 2. Particles of varying shapes are made by using a combination of stretching and liquefying

(A) Ribbons with curled ends; **(B)** bicones; **(C)** diamond disks; **(D)** emarginated disks; **(E)** flat pills; **(F)** elongated hexagonal disks; **(G)** ravioli; **(H)** tacos; **(I)** wrinkled prolate ellipsoids; **(J)** wrinkled oblate ellipses; and **(K)** porous elliptical disks.

Reprinted with permission from [49]. © National Academy of Sciences of the USA, *PNAS* (2007).

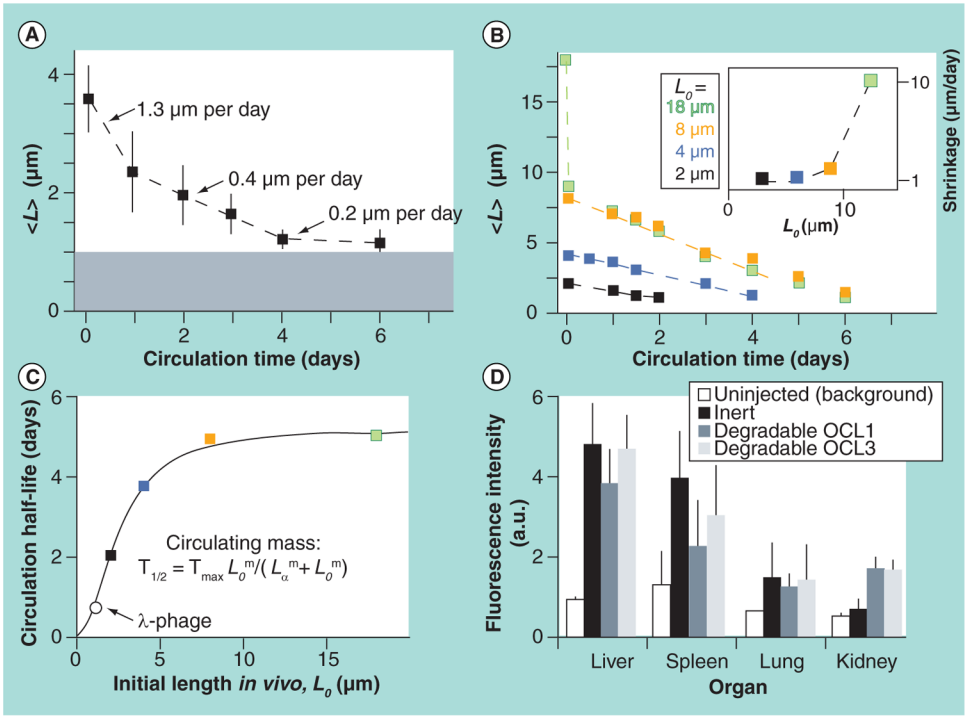

Figure 3. Kinetics of filomicelle of various lengths *in vivo*

(A) The length of inert filomicelles shortens with the circulation time. The optical diffraction limit of length measurements is marked by the grey region. **(B)** The initial length of the degradable filomicelles (OCL3) determines its shortening rate (Inset plot: length dependent shrinkage rate). **(C)** A saturable increase in half-life of circulating mass is exhibited by filomicelles, fitting a cooperative clearance model with τ_{max} = 5.2 days, m = 2.1 and L_o = 2.5 μm. **(D)** The distribution of inert and degradable filomicelles in clearance organs (L_o = 4 or 8 μm after 4 days of circulation in rats).

OCL: Polyethylene glycol-polycaprolactone assembled polymersomes.

Reprinted by permission from [15]. © Macmillan Publishers Ltd. *Nature* (2007).

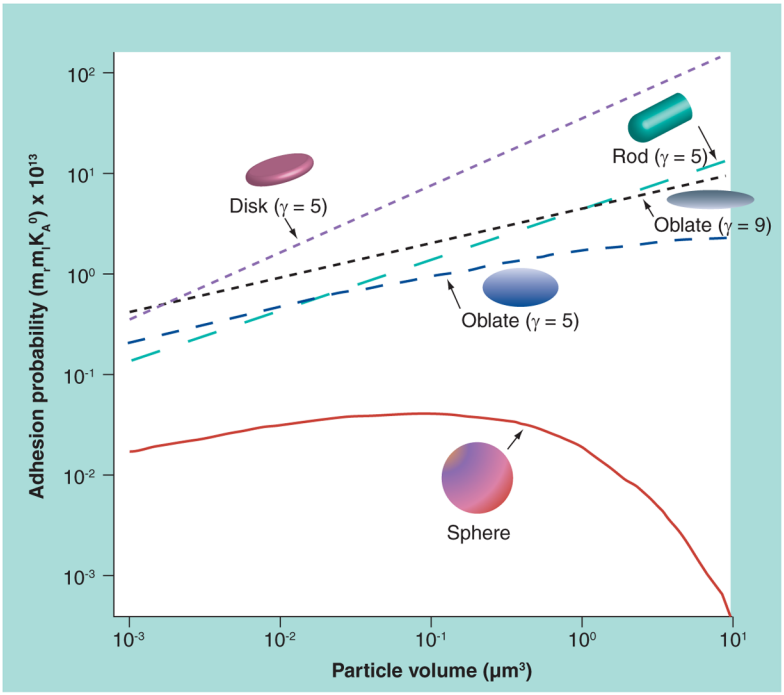

Figure 4. Adhesion probabilities of nanoparticles of various shapes as a function of particle volume

γ is the aspect ratio.

Reprinted with permission from [71]. © The Royal Society of Medicine Press Ltd, *Exp. Biol. Med.* (2011).

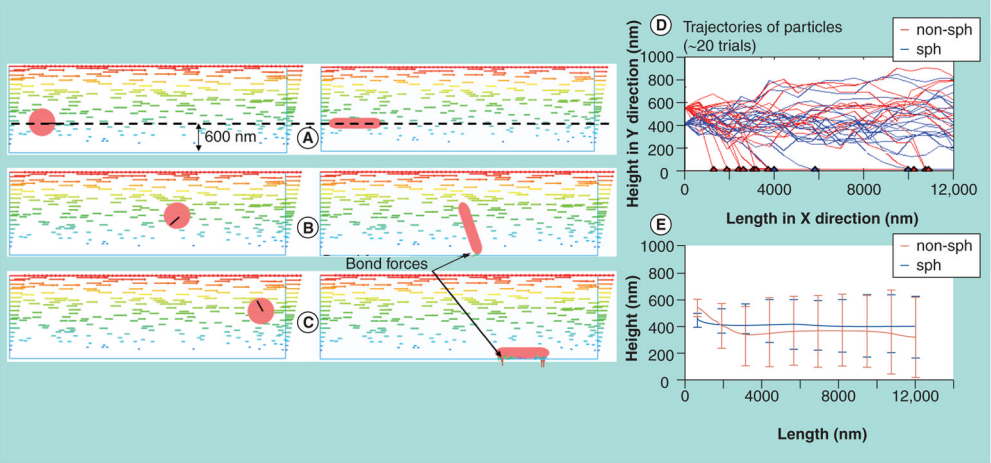

Figure 5. Shape-dependent particle adhesion kinetics

The left column of **(A)**, **(B)** and **(C)** shows a spherical particle washed away without contact with surface; Right hand column of **(A)**, **(B)** and **(C)** shows a nanorod tumbles and gets deposited. **(A)**, **(B)** and **(C)** are at times t = 0, 0.5 and 0.75 s, respectively. The line labeled on the spherical particle indicates its rotation. The horizontal arrows in fluid domain indicate the fluid field. Arrows shown on nanoparticles indicate the magnitude and direction of bonding forces. Right column shows comparing trajectories of nanorod and nanosphere to study shape effect on particle adhesion kinetics. **(D)** Trajectories of 20 independent trials of nanorod and nanosphere, where red spot indicates adhesion of nanorod and blue spot indicates adhesion of nanosphere at that location. **(E)** Mean trajectory of 20 trials of nanorod and nanosphere with standard deviation shown as vertical bar.

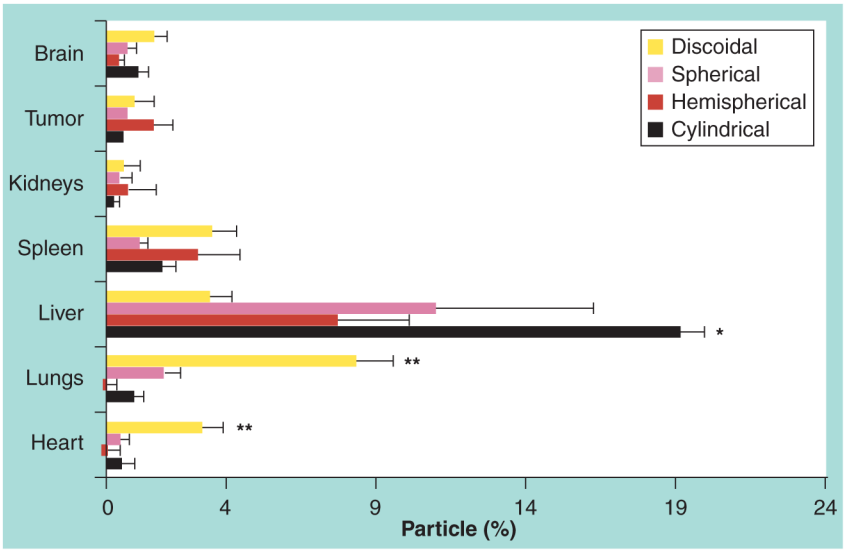

Figure 6. *In vivo* silicon accumulation in various organs relative to the injected dose for nonspherical particles

The percentage of silicon in each organ corresponds to the number of particles. The difference between the discoidal and the other particles with $p < 0.001$ is represented by the star symbol.

Reprinted with permission from [74]. © Elsevier (2010).

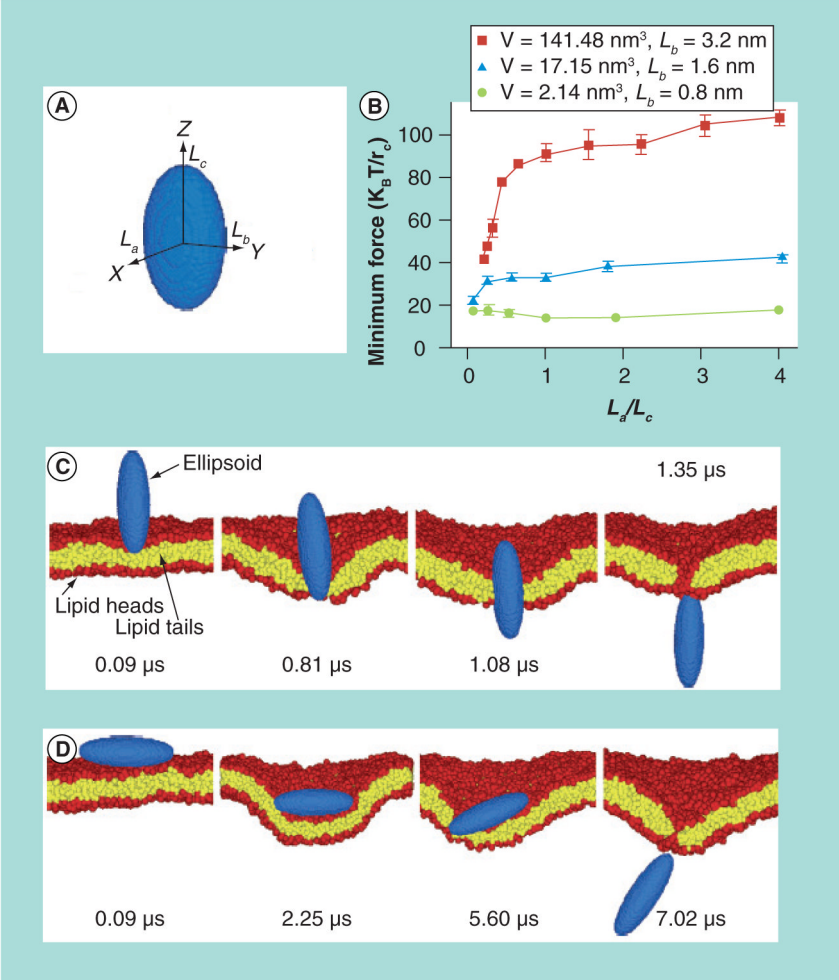

Figure 7. Penetration of ellipsoidal nanoparticles with different shapes across a lipid bilayer

(A) Ellipsoid particle, where L_a, L_b and L_c represent the half-lengths of the three axes. **(B)** Minimum driving forces required to attract ellipsoids of different volumes through the lipid bilayer. By varying the aspect ratio, the shape anisotropy of the particles are adjusted (L_a/L_c) at fixed L_b and volume. **(C**,**D)** Computer-simulated diagram showing the translocation of ellipsoids with **(C)** vertical and **(D)** horizontal starting orientations. L_a = 1.6 nm, L_b = 3.2 nm and L_c = 6.4 nm for **(C)**, and L_a = 6.4 nm, L_b = 3.2 nm and L_c = 1.6 nm for **(D)**. Reprinted with permission from [77]. © Nature Publishing Group (2010).

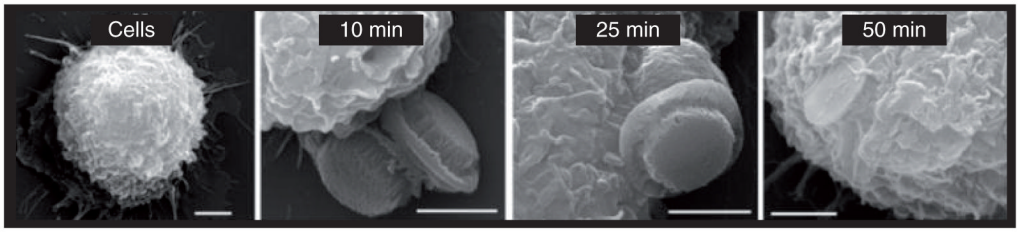

Figure 8. Cellular engulfment of silicon microparticles (S1MPs) by J774A.1 macrophages
Scanning electron microscope images of J444A.1 cells incubated with S1MPs (at a ratio of 1:5) for different lengths of time demonstrating particle orientation during uptake and varying degrees of internalization (10, 50, 50 and 40 k).
Reprinted with permission from [78]. © John Wiley & Sons (2010).

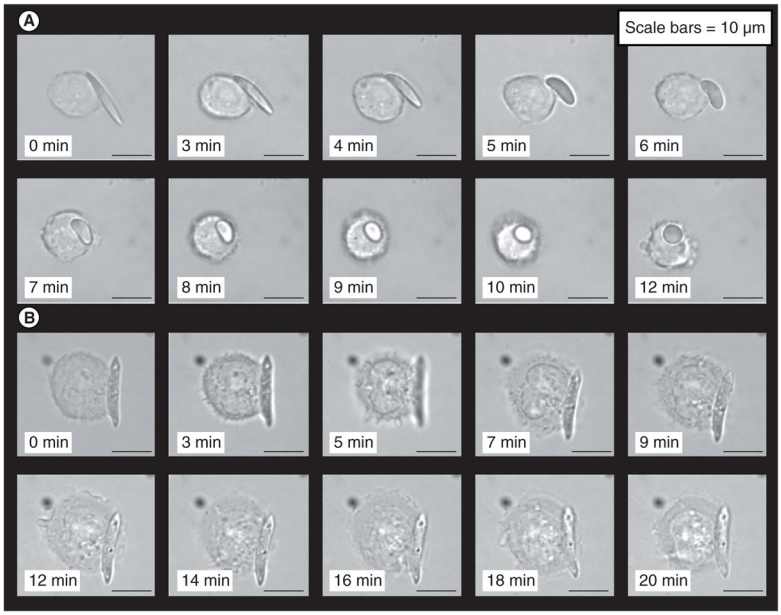

Figure 9. Shape-dependent phagocytosis by macrophage recorded using time-lapse video microscopy

(A) Shape-switching poly(lactic-co-glycolic acid) (PLGA)-ester elliptical disk (mixture of two PLGAs, AR = 5) quickly being phagocytized and internalized by the macrophage as the particle switches to near-spherical shape. **(B)** Macrophage spreads on a PLGA-acid elliptical disk (molecular mass 4.1 kDa, T_g[mid] = 27°C, AR = 5), but could not complete phagocytosis. Particle does not switch shape at pH 7.4.

Reprinted with permission from [102]. © National Academy of Sciences of the USA, *PNAS* (2010).

Table 1

Nanoparticles of various shapes fabricated in recent years.

Method	Size	Shape	Material	Application	Ref.
PRINT®	10 nm to μm size	Cube, rod, circular disc, cone and hexagon	Poly(ethylene glycol diacrylate), triacrylate resin, PLA and poly(pyrrole)	Therapeutic vectors and diagnostic imaging agent carriers	[47,48]
Stretching spherical particles	60 nm to 30 μm	Sphere, rod, circular/elliptical disc, oblate/prolate ellipsoid and worm	Polystyrene and poly(D,L-lactic acid-co-glycolic acid	Drug delivery, medical imaging, advanced materials and microfluidics	[49,50]
Step flash imprint lithography	50 nm	Cube and triangular/pentagon cylinder	polyethylene glycol dimethacrylate and poly(ethylethylene glycol diacrylate-co-acrylated Gly-Phe- Leu-Gly-Lys)	DNA plasmid release and drug delivery	[51]
Self-assembled	L = a few μm, D = 20–60 nm	Long worm shape	Copolymers and PEG	Drug delivery	[15]
Layer-by-layer self-assembly technique	7 ± 2 μm	Red blood cell shaped	BSA and PAH	Drug delivery	[30]
Template-induced printing	80 nm	Circular disc, long worm, bullet and rod	SU-8, PEGDA and poly(ethylene glycol)-co-poly(D,L-lactic acid)	Drug delivery	[54]

BSA: Bovine serum albumin; PAH: Poly(allylamine hydrochloride); PEG: Polyethyleneglycol; PEGDA: PEG diacrylate; PLA: Poly(lactic acid).